Model quantum magnet: The effect of hyperfine interactions on the phase diagram and dynamic susceptibility

Varsha Banerjee[1,*] and Sushanta Dattagupta[2,†]
[1]*Department of Physics, Indian Institute of Technology, Hauz Khas, New Delhi 110016, India*
[2]*S. N. Bose National Centre for Basic Sciences, J. D. Block, Salt Lake, Sector III, Calcutta 700098, India*
(Received 22 January 2001; published 22 June 2001)

We study the effect of hyperfine interactions on static and dynamic properties of a model quantum magnet. A mean field theory of the transverse Ising model with an additional hyperfine interaction term agrees rather well with the experimentally obtained phase diagram and dynamic susceptibility measurements in $LiHoF_4$ which of late, is being referred to as a model quantum magnet.

DOI: 10.1103/PhysRevB.64.024427 PACS number(s): 75.10.Dg

I. INTRODUCTION

Magnetism has continued to remain a topic of great interest in condensed matter physics due to its impact on our understanding of cooperative behavior and on technological applications. Of late, there has been widespread interest in the role of quantum fluctuations on the phase transition properties of ideal magnets. At high temperatures (close to the critical temperature), the system can access different minima of the free energy by thermal activation processes. At low temperatures, however, the mechanism of relaxation is quantum mechanical, due to tunneling between different minima of the free energy surface. Since the thermal activation processes die out as the temperature is lowered, tunneling through barriers due to quantum fluctuations becomes dominant as they do not vanish when the temperature approaches zero.

All finite-temperature transitions are considered to be classical. This is so, because even in quantum systems (such as a superconductor) sufficiently close to the critical temperature, quantum fluctuations are important at microscopic length scales but not at the longer length scales that control the critical behavior. Of course, quantum mechanics is needed for the very existence of an order parameter, but it is the classical thermal fluctuations that govern it at long wavelengths. Therefore, a Landau-Ginzburg-type theory is adequate for describing the phase transition. At low temperatures, however, quantum tunneling plays the role of a disordering field such as temperature. Thus, even at zero temperature, one can induce an order-disorder phase transition by tuning the quantal fluctuations. This phenomenon is called a quantum phase transition because it occurs due to purely quantum fluctuations. It takes place at $T=0$. Crossing the phase boundary implies some fundamental changes in the quantum ground state.[1]

Second-order phase transitions are accompanied by a divergent correlation length and correlation time, i.e., the order parameter fluctuates coherently over increasing distances and ever more slowly. The latter implies that there is a frequency ω^* associated with critical fluctuations that goes to zero at the transition. Therefore a quantum system behaves classically if the frequency-scale associated with the temperature exceeds all frequencies of interest, including ω^*. Since $\hbar\omega^* \ll k_B T_c$, close to the transition, the critical fluctuations behave classically. Thus quantum phase transitions, where $T_c=0$ are qualitatively different and their critical fluctuations must be treated quantum mechanically.

Quantum phase transitions differ fundamentally from classical phase transitions and fall in a new universal class of critical phenomena. The fascinating properties of a variety of systems involving transition metal oxides,[2] the apparent ''non-Fermi liquid'' behavior of highly correlated *f*-electron compounds,[3,4] and the unusual normal-state properties of the high T_c superconducting cuprates have all been attributed to the closeness of the quantum critical point. This class of problems is presently an active area of research.[5]

Although there is tremendous interest in high-precision and controlled investigation of quantum critical phenomena, unambiguous study of these systems is quite difficult, partly because it is not always straightforward to define an order parameter. There are only a few such systems that have been subjected to careful experimental investigation. Fortunately, one such system is the recently much-investigated[6] dipolar coupled ferromagnet $LiHoF_4$. In fact, so well can the quantum phase transition be studied in this system, that it is being referred to as a model quantum magnet. The experimentally measured critical temperature, for transition from the paramagnetic to the ferromagnetic phase, in the absence of quantal fluctuations, is $T_c=1.53$ K. In the experiments of Bitko, Rosenbaum, and Aeppli[6] a small magnetic field transverse to the *c* axis is applied in the laboratory that causes an admixture of the ground-state doublet. The transverse field induces quantum fluctuations and is the disordering field responsible for the quantum phase transition in the model magnet $LiHoF_4$. An experimental phase boundary for the ferromagnetic transition in the transverse field–temperature plane has been obtained by Bitko, Rosenbaum, and Aeppli via magnetic susceptibility measurements. They calculated the mean-field phase boundary using a Hamiltonian comprising of the electronic spin degrees of freedom of Ho^{3+}. The calculated phase boundary agreed well with experimental measurements for values of temperature larger than 0.6 K. However, there was substantial deviation from experimental results at lower temperatures near the quantum phase transition. A further calculation involving the full Hamiltonian of the Ho^{3+} ion with its 136 basis states (arising out of the 17 electronic

states) and eight nuclear states (to account for the hyperfine coupling between Ho nuclear spins with electrons) gave an accurate match for all values of temperature. These calculations underscore the importance of hyperfine interactions, especially at temperatures close to the quantum critical point. It is precisely this important issue that we focus on in this paper and discuss its relevance on the static and dynamic properties of $LiHoF_4$.

While the computation of the phase boundary is reasonably tractable even though the basis states of the full Hamiltonian are large in number, the calculation of dynamic susceptibility becomes a very complex issue. As the imaginary part of the frequency-dependent susceptibility is associated with dissipation, any treatment of dynamics has to necessarily take into account the various relaxation processes. This becomes an insurmountable problem if the Hilbert space of the ''free'' Hamiltonian is as large as in the present instance (comprising of 136 states). We, however, represent the holmium moments by Ising spins making use of the fact that at low operating temperatures of $LiHoF_4$, only the two lowest crystal-field-split levels are predominantly occupied. Thus the dipolar interaction between holmium moments can be adequately described by an Ising Hamiltonian. For the same reason and for the fact that the uniaxial (along the Ising easy axis) component of the g tensor is atleast an order of magnitude larger than the transverse component, the hyperfine interaction tensor can be assumed diagonal. How good this approximate model is can be tested by first computing the static phase diagram, in this mean field theory. We find a good agreement with the experimental as well as analytical results of Bitko, Rosenbaum, and Aeppli. Bolstered by this, we extend our model to calculate the frequency-dependent susceptibility for the model quantum magnet using a system-plus-bath approach. It is to our satisfaction that we find that the results derived for the dynamic susceptibility are also in qualitative agreement with experimental measurements on $LiHoF_4$.

The outline of the paper is as follows. In Sec. II we introduce the Hamiltonian for the model quantum glass. The mean field theory is discussed in Sec. III. The static properties, viz., the phase diagram and the static susceptibility evaluated from the mean field equations are discussed in Sec. IV. Section V is devoted to a discussion of relaxation phenomena in thermal equilibrium in terms of the dynamic susceptibility. The results and discussion relevant to this calculation are presented in Sec. VI. Finally in Sec. VII, we present a few concluding remarks.

II. THE HAMILTONIAN

The transverse Ising model (TIM) occupies a special position in statistical mechanics not only because so many of its properties have been extensively studied, but also because of its wide applicability to condensed matter physics. A very recent application of the TIM involves the dipolar coupled $LiHoF_4$ quantum magnet. The system $LiHoF_4$ belongs to a class of compounds $LiRF_4$, where R is a rare-earth element. The rare-earth moments of Ho^{3+} are essentially dipolar coupled, but because of the presence of large crystal field, only the lowest Kramers doublet of the 17 crystal-field-split states is appreciabely populated at low temperatures ($T<2$ K). Further, the sign of the crystal field is negative, hence the lowest doublet corresponds to the highest spin substates. Consequently, the off-diagonal terms of the dipolar interaction are effectively ''quenched,''[7] yielding the so-called ''truncated dipolar Hamiltonian.''[8] The latter leads to the Ising form of interaction amongst the spins along the crystallographic c axis. In the experiments of Bitko, Rosenbaum, and Aeppli, a small magnetic field transverse to the c axis is applied in the laboratory that causes the admixture of the crystal-field-split doublet. Since this field couples to the component of the spin perpendicular to the c axis, the transverse Ising model provides a valid description of the statistical mechanics of the system. Keeping in mind the relevance of hyperfine interactions near the quantum phase transition of $LiHoF_4$, our starting point is the Hamiltonian for the TIM including hyperfine interaction:

$$H_s = -\sum_{i,j=1}^{N} J_{ij}\sigma_i^z\sigma_j^z - \sum_{i=1}^{N} aI_i^z\sigma_i^z - \Omega\sum_{i=1}^{N}\sigma_i^x. \qquad (1)$$

Here, J_{ij} is the interaction between the Ising spins which, recalling its origin in dipolar coupling, is given by[8,9]

$$J_{ij} = g^2\mu^2[1-3\cos^2(\theta_{ij})]/r_{ij}^3, \qquad (2)$$

where g is the gyromagnetic ratio, μ is the Bohr magneton, and r_{ij} and θ_{ij} are respectively the magnitude and the polar angle of the vector $(\overline{r_i}-\overline{r_j})$ connecting sites i and j with respect to the c axis. The radial dependence, $1/r_{ij}^3$ means that the dipolar interaction is long ranged in nature and many more than nearest-neighbor interactions must be taken into account. The angular dependence $[1-3\cos^2(\theta_{ij})]$ implies that J_{ij} can change sign, and hence the interaction switches from ferromagnetic for angles close to the Ising axis to antiferromagnetic for intermediate angles ($55°\leqslant\theta_{ij}\leqslant 125°$). While the occurrence of competing interactions can raise doubt on the uniqueness of the ground state, a classical analysis by Luttinger and Tisza had shown that the ground state is that of a dipolar ferromagnet.[10]

The second term in Eq. (1) represents the hyperfine interaction between the nuclear spin I_i^z and the electronic spin σ_i^z of Ho^{3+}. It arises from the interaction of the Ho nuclear spins with the electronic states through a core polarization effect[11] and its practical relevance for the magnetic ordering in quantum magnets is well understood.[12] ''a'' is a hyperfine coupling constant, which for $LiHoF_4$ is 0.039 K (Refs. 11 and 13). Normally, the hyperfine interaction is isotropic. But for the same reasons of anisotropy mentioned before, which lead to the truncated form of the dipolar interaction, the off-diagonal components of the hyperfine interaction are also effectively quenched. This explains the form of the hyperfine interaction written in Eq. (1) that involves only the z component (i.e., along the c axis) of the nuclear and electronic spins.

The third term in Eq. (1) induces tunneling effects by mixing the eigenstates of the σ^z operator, thus introducing quantum dynamics in the system. In the experiments of

Bitko, Rosenbaum, and Aeppli, this is realized by the application of a magnetic field H_t perpendicular to the c axis. This field can cause an admixture of the crystal-field-split states yielding in perturbation theory a spin Hamiltonian that depends on σ_x with a prefactor Ω that is quadratic in H_t^2. The transverse field Ω plays the role of a disordering field, like the temperature T. This is because as Ω increases, it causes an increasingly large amount of energy for the spins to order along the z axis. Thus, even at zero temperature there is a critical value Ω_c such that for $\Omega > \Omega_c$ the system goes into a paramagnetic phase resulting in a quantum phase transition.

With this background, it is evident that the Hamiltonian described by Eq. (1) provides a valid theoretical framework to study the static properties of the model quantum magnet $LiHoF_4$. The long-range nature of the dipolar interaction makes this Hamiltonian a suitable candidate for a mean field analysis to evaluate the physical properties of the system. In the next section, we discuss the mean field theory for the model and study the static properties. In fact, we will show that the mean field theory works rather well in understanding the experimental results at a qualitative level.

III. MEAN FIELD THEORY

The basic idea of the mean field theory is to isolate a given spin, say the ith one, and embed it in an effective medium in which the local field at the ith site is given (self-consistently), by the expectation value of the spin operator itself. Thus, in the mean field approximation, the Hamiltonian in Eq. (1) can be rewritten as

$$H_s = -\sum_{i=1}^{N} (aI_i^z + H_i)\sigma_i^z - \Omega \sum_{i=1}^{N} \sigma_i^x, \tag{3}$$

where

$$H_i = \sum_{j=1}^{N} J_{ij} \langle \sigma_j^z \rangle. \tag{4}$$

Further, in the ''uniform'' case, $\langle \sigma_j^z \rangle$ is independent of the site index j, yielding $H_i = H = J(0)\langle \sigma^z \rangle$ where $J(0) = \Sigma_j J_{ij}$. The single-site Hamiltonian is thus

$$H_s = -(aI^z + H)\sigma^z - \Omega \sigma^x. \tag{5}$$

The partition function is given by

$$Z = \mathrm{Tr}(e^{-\beta H_s}) = [\mathrm{Tr} \exp\{\beta[(aI^z + H)\sigma^z - \Omega\sigma^x]\}]^N, \tag{6}$$

N being the number of sites. The trace in Eq. (6) is over the electronic as well as the nuclear spin eigenstates. Labeling the eight nuclear eigenstates by $|M\rangle$, we have $I^z|M\rangle = M|M\rangle$, $M = -\frac{7}{2} \ldots \frac{7}{2}$. Thus the partition function Z can now be written as

$$Z = \left[\sum_{M=-7/2}^{7/2} \mathrm{Tr} \exp\{\beta[(aM + H)\sigma^z - \Omega\sigma^x]\} \right]^N, \tag{7}$$

where the trace now is over the eigenstates of the electronic spins σ^z alone. Using the property of Pauli matrices, Eq. (7) can be simply rewritten as

$$Z = \left[\sum_{M=-7/2}^{7/2} \cosh\{\beta h(M)\} \right]^N, \tag{8}$$

where

$$h(M) = \sqrt{(aM + H)^2 + \Omega^2}. \tag{9}$$

On the other hand, the magnetization $\langle \sigma^z \rangle$ is given by

$$\langle \sigma^z \rangle = \frac{\mathrm{Tr}[\sigma^z \exp\{\beta[(aI^z + H)\sigma^z - \Omega\sigma^x]\}]}{\sum_M \cosh[\beta h(M)]}, \tag{10}$$

where the trace, once again, is over both nuclear and electronic eigenstates. Taking trace and writing $\langle \sigma^z \rangle = m^z$ and $H = J(0)m^z$ we can rewrite Eq. (10) as

$$m^z = \frac{\sum_M \frac{aM + J(0)m^z}{h(M)} \sinh[\beta h(M)]}{\sum_M \cosh[\beta h(M)]}. \tag{11}$$

Equation (11) gives the self-consistent relation for the z component of magnetization. It is evident that m^z goes to zero in the limits of either Ω or T approaching infinity. Thus the transverse field Ω, like the temperature T, plays the role of a disordering field. The terms in Eq. (11) can be rearranged as to give

$$1 = \frac{\sum_M \frac{1}{\beta h(M)} \left[\frac{\beta a M}{m^z} + \beta J(0) \right] \sinh[\beta h(M)]}{\sum_M \cosh[\beta h(M)]}. \tag{12}$$

We now proceed to evaluate the phase boundary separating the ferromagnetic and the paramagnetic phases of the model system in the T-Ω plane. Since m^z is small near the phase boundary, Eq. (9) can be approximated as

$$h(M) = h_0(M) + \alpha(M)m^z, \tag{13}$$

where $h_0(M) = \sqrt{a^2M^2 + \Omega^2}$ and $\alpha(M) = aMJ(0)/h_0(M)$. With this approximation, Eq. (12) can be rewritten as

$$1 = \frac{\sum_M \frac{\Omega^2 J(0)}{(a^2M^2 + \Omega^2)^{3/2}} \sinh(\beta\sqrt{a^2M^2 + \Omega^2}) + \frac{\beta J(0) a^2 M^2}{a^2M^2 + \Omega^2} \cosh(\beta\sqrt{a^2M^2 + \Omega^2})}{\sum_M \cosh[\beta h(M)]}. \tag{14}$$

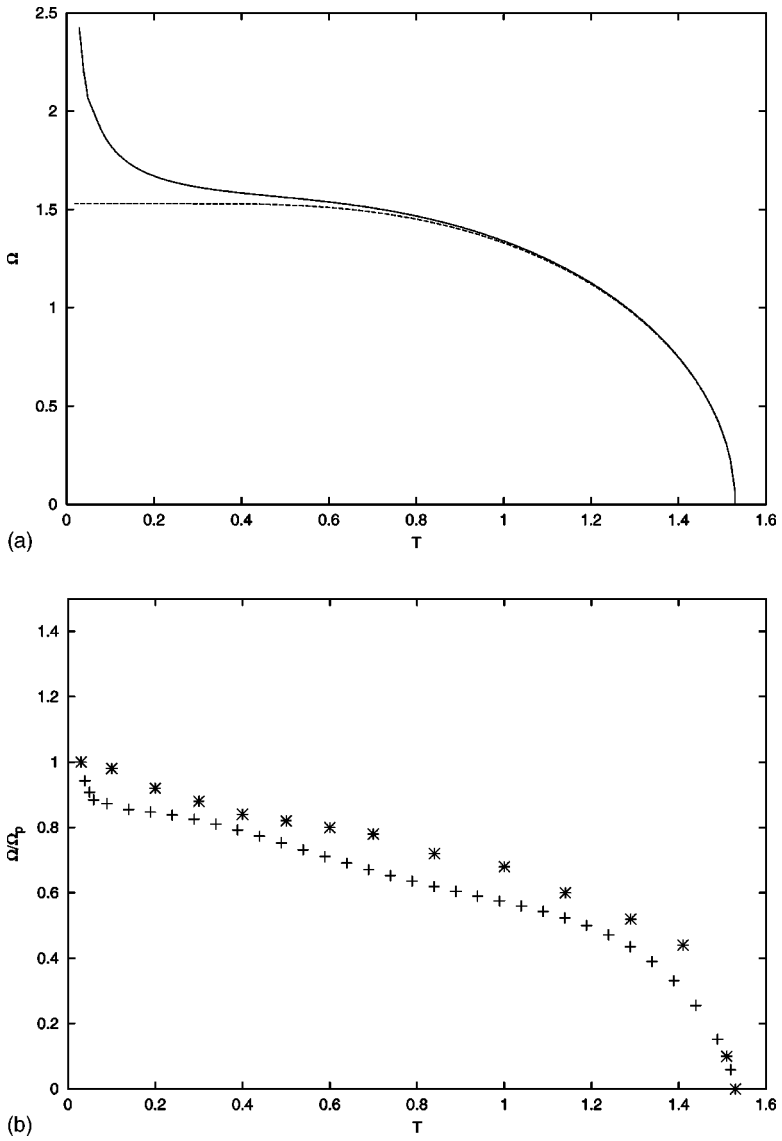

FIG. 1. (a) Numerical evaluation of the phase boundary separating the ferromagnetic phase from the paramagnetic one using Eq. (14) (solid curve). The phase boundary computed in the absence of hyperfine interaction (dashed curve) is also shown for comparison. 1(b) Comparison between experimentally obtained phase boundary of Bitko, Rosenbaum, and Aeppli (stars) from susceptibility measurements and our calculated mean-field phase boundary (pluses) in the presence of hyperfine interactions. The data have been scaled by the respective maximum values of the transverse field in each case.

This is the main equation for our study of the static properties of the model quantum magnet. In the limit $a=0$, we get the expected answer with the phase boundary being given by

$$1=\frac{J(0)}{\Omega}\tanh(\beta\Omega), \tag{15}$$

which in the $\Omega\to 0$ limit gives us the value of $J(0)=1/\beta_c = k_B T_c^0$. As mentioned earlier, the critical temperature of the dipolar magnet in the absence of the transverse field Ω, T_c^0, is 1.53 K.

IV. STATIC PROPERTIES

(i) Phase boundary: The numerical evaluation of the phase boundary seperating the ferromagnetic phase from the paramagnetic one, evaluated using Eq. (14), is shown in Fig. 1(a). For comparison, we have also shown the phase boundary computed from Eq. (15) (dashed curve), in the absence of the hyperfine interaction. In Fig. 1(b), we bring out the comparison between the experimentally obtained phase boundary of Bitko, Rosenbaum, and Aeppli (stars) from susceptibility measurements and our calculated mean field phase boundary (pluses) in the presence of hyperfine interactions. The data have been scaled by the largest value of Ω for comparison. The good qualitative agreement with experimental data provides credence to the Ising approximation of the model and its mean field treatment.

To understand the qualitative difference in the phase boundary in the presence of hyperfine interactions in Fig. 1, we consider different limiting situations.

(1) For $\Omega=0$, Eq. (14) yields

$$1=\frac{\sum_M \beta_c J(0)\cosh(\beta a M)}{\sum_M \cosh(\beta a M)}=\beta_c J(0). \tag{16}$$

Thus, T_c^0 is unaffected by the hyperfine interaction.

(2) In the region $\Omega > a$, Eq. (14) reduces to

$$1=\frac{J(0)}{\Omega}\tanh(\beta\Omega)+\frac{\beta J(0)a^2}{\Omega^2(2I+1)}\sum_M M^2. \tag{17}$$

Furthur, if we consider low temperatures, Eq. (17) can be further approximated as

$$1=\frac{J(0)}{\Omega}+\frac{\beta J(0)a^2}{\Omega^2(2I+1)}\sum_M M^2. \tag{18}$$

Writing Ω/k_B as $\bar{\Omega}$, a/k_B as $\bar{a}$ and $\Sigma_M M^2/(2I+1)=\gamma$, we obtain a quadratic in $\bar{\Omega}$

$$\bar{\Omega}^2-\bar{\Omega}T_c^0-\gamma\frac{T_c^{0^2}}{T_c}\bar{a}^2=0, \tag{19}$$

which to first order in T_c^0 yields

$$\bar{\Omega}_c=T_c^0+\gamma\frac{\bar{a}^2}{T_c}. \tag{20}$$

Thus we have an enhancement of T_c in the presence of hyperfine interactions when (a) Ω is large as compared to a and (b) the temperatures are close to the quantum critical point.

The increment in Ω_c can also be understood from the following physical argument. For small values of the transverse field, the local mean-field is dominated by the effective interaction proportional to the magnetization along the c axis. However, as the transverse field increases, the magnetization along the c axis goes on decreasing (because of the gradual loss of the quantization axis) leading to a situation in which the local field is dominated by the hyperfine coupling alone. Thus, the ferromagnetic order persists for larger values of the transverse field as temperature approaches zero. Hence, as also observed by Bitko, Rosenbaum, and Aeppli, there is a characteristic upward tilt in the phase boundary for temperatures less than 0.6 K.

(ii) Static susceptibility: The static susceptibility can be calculated by adding a small magnetic field ΔH along the z axis. The average magnetization m^z in the presence of the field is

$$m^z=\frac{\sum_M \frac{aM+\tilde{H}}{h(M)}\sinh[\beta h(M)]}{\sum_M \cosh[\beta h(M)]}, \tag{21}$$

where $\tilde{H}=H+\Delta H$ and $h(M)=\sqrt{(aM+\tilde{H})^2+\Omega^2}$. Now, in the paramagnetic phase, H is small, hence $\tilde{H}$ is also small. In this limit, we can expand $h(M)$ in powers of $\tilde{H}$, retaining only the first-order terms. Writing $\tilde{H}=J(0)m^z+\Delta H$, we obtain from Eq. (21)

$$m^z[1-J(0)X]=\Delta H X. \tag{22}$$

The static susceptibility is thus

$$\chi=\frac{X}{1-J(0)X}, \tag{23}$$

where

$$X=\frac{\sum_M \frac{1}{h_0(M)^3}\{\Omega^2\sinh[\beta h_0(M)]+\beta a^2M^2h_0(M)\cosh[\beta h_0(M)]\}}{\sum_M \cosh[\beta h_0(M)]}. \tag{24}$$

The static susceptibility evaluated as a function of the transverse field Ω is shown in Fig. 2. We have selected the temperature to be 0.19 K, where the hyperfine interaction term is dominant. For comparison, we show the variation of susceptibility for the case when the hyperfine interaction term is included (solid line) and for the case when it is not included (dashed line). In both situations, a cusp in the static susceptibility is observed at corresponding values of the critical fields for the selected temperature of 0.19 K, indicative of a phase transition. The inset shows a double logarithmic plot of the susceptibility as a function of $|1-\Omega/\Omega_c|$ to bring out the clear distinction between the divergences when hyperfine interactions are included (solid line) and when they are not (dashed line).

V. DYNAMIC SUSCEPTIBILITY

We now focus our attention on the evaluation of dynamic properties in terms of the frequency-dependent electronic susceptibility of the model quantum magnet. The Hamiltonian of Eq. (5) describes the reversible quantum dynamics of the system. Although it leads to interesting physics by itself, we now discuss irreversible effects to include dissipative dynamics in the system. The irreversibility can be studied by including a coupling to the surrounding heat bath in Eq. (5)

$$H_0=H_S+H_I+H_B, \tag{25}$$

where H_I describes the interaction between the spin system and the heat bath. This term needs to be selected appropriately. In order to find the correct expression for H_I it is useful to first diagonalize H_S by rotating the coordinate system about the y axis in a clockwise direction by an angle $\theta=\arctan(\Omega/h)$. The corresponding rotation operator in the spin space of the subsystem is

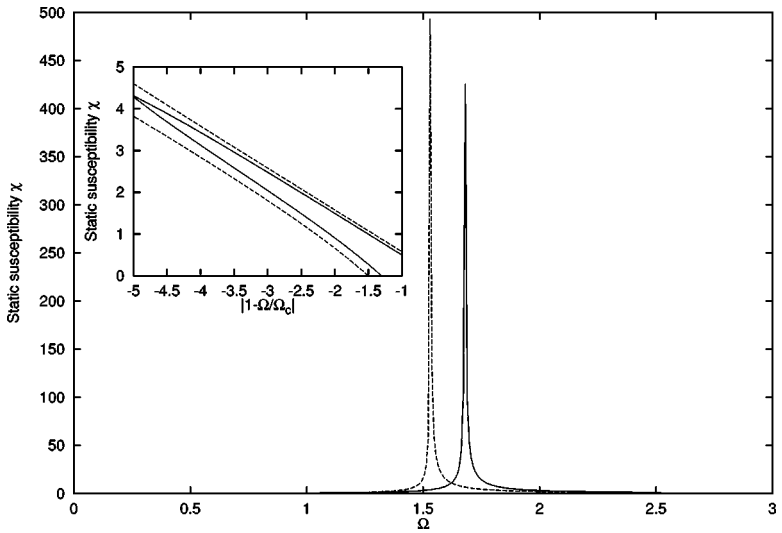

FIG. 2. Static susceptibility as a function of the transverse field Ω at $T=0.19\,\mathrm{K}$, where the hyperfine interaction is dominant. The solid line corresponds to evaluation of χ in the presence of hyperfine interactions, while the dashed line corresponds to the evaluation in the absence of hyperfine interactions. The inset is a log-log plot of the same data to distinguish between divergence near the transition point in the two distinct cases.

$$U_Y^R = e^{-i\theta\sigma^y}. \tag{26}$$

In the rotated frame, the total Hamiltonian is

$$\tilde{H}_0 = \tilde{H}_S + \tilde{H}_I + H_B, \tag{27}$$

while the subsystem Hamiltonian H_S, which is now diagonal, is given by

$$\tilde{H}_S = h_0\sigma^y. \tag{28}$$

The effective field h_0 is

$$h_0 = \sqrt{(aI^z+H)^2+\Omega^2}. \tag{29}$$

There is always the issue: what should be the form of the interaction term H_I? We make the following choice as given in Eq. (30) and provide the rationale below:

$$\tilde{H}_I = gb\sigma^x. \tag{30}$$

In Eq. (30), b is a heat-bath operator that acts on the Hilbert space of the bath Hamiltonian H_B and g is a multiplicative coupling constant. The specific form of interaction that we have chosen [see Eq. (30)] guarantees that in the rotated frame in which H_S is diagonal, the coupling with the heat bath is purely off-diagonal, i.e., H_I involves σ^x alone and is known to yield thermal fluctuations as in the Glauber model.[14] Unrotating Eq. (30), we find, in the laboratory frame,

$$H_I = \frac{gb}{h_0}[(aI^z+H)\sigma^x - \Omega\sigma^z]. \tag{31}$$

It is evident that when tunneling is absent (i.e., $\Omega=0$), H_S reduces to the Ising Hamiltonian in the mean-field approximation and the coupling to the heat bath assumes the form of Eq. (30). In this limit, we recover the Glauber kinetics for the ordinary Ising model. Thus we see that the full interaction term provides spin flips of the Glauber type via σ^x and incoherent tunneling effects via σ^z, if we choose z, the Ising easy axis as the axis of quantization.

We now turn our attention to the evaluation of the frequency-dependent dynamic susceptibility $\chi(\omega)$. This, in linear response theory, adapted to single-site mean-field approximation, is given by[15]

$$\chi(\omega) = \beta \lim_{\delta\to 0, s\to -i\omega+\delta} [1 - s\tilde{C}(s)], \tag{32}$$

where $\tilde{C}(s)$ is the Laplace transform of the correlation function defined as

$$C(t) = \langle \sigma^z(0)\sigma^z(t)\rangle_{\mathrm{eq}}. \tag{33}$$

Here the angular brackets denote the appropriate quantum and statistical average. The quantity s is related to the applied frequency ω, δ is a small real-valued parameter to ensure convergence of Laplace transforms, and β is the inverse temperature. $C(t)$ can be explicitly written in the equillibrium ensemble as

$$C(t) = \mathrm{Tr}(\rho_{\mathrm{eq}}\sigma^z(0)e^{iH_0t}\sigma^z(0)e^{-iH_0t}), \tag{34}$$

where H_0 is the total Hamiltonian as in Eq. (25) and Z_0 is the corresponding partition function. In the rotated frame the correlation function reads

$$C(t) = \mathrm{Tr}\left(\tilde{\rho}_{\mathrm{eq}}\left[\frac{(aI^z+H)}{h_0}\sigma^z - \frac{\Omega}{h_0}\sigma^x\right]e^{i\tilde{H}_0t}\left[\frac{(aI^z+H)}{h_0}\sigma^z - \frac{\Omega}{h_0}\sigma^x\right]e^{-i\tilde{H}_0t}\right), \tag{35}$$

where $\tilde{H}_0$ is the total Hamiltonian in the rotated frame, as given by Eq. (27). Assuming that the subsystem is weakly coupled to the heat bath, we can factorize the density matrix and write the correlation function as

$$C(t) = \frac{1}{Z_s}\mathrm{Tr}(A),$$

$$A=e^{-\beta\tilde{H}_s}\left[\frac{(aI^z+H)}{h_0}\sigma^z-\frac{\Omega}{h_0}\sigma^x\right]\mathrm{Tr}_B\left\{\frac{e^{-\beta H_B}}{Z_B}\left(U(t)\times\left[\frac{(aI^z+H)}{h_0}\sigma^z-\frac{\Omega}{h_0}\sigma^x\right]\right)\right\}. \quad (36)$$

The trace, as before is over the Ising spin states as well as the nuclear spin states and Tr_B is over the bath degrees of freedom alone. $[U(t)]$ is the time development operator to be computed with the aid of the total Hamiltonian given by Eq. (27). The Laplace transform of $C(t)$ reads

$$\tilde{C}(s)=\frac{1}{Z_s}\mathrm{Tr}\left(e^{-\beta\tilde{H}_s}\left[\frac{(aI^z+H)}{h_0}\sigma^z-\frac{\Omega}{h_0}\sigma^x\right]\times[\tilde{U}(s)]_{\mathrm{av}}\left[\frac{(aI^z+H)}{h_0}\sigma^z-\frac{\Omega}{h_0}\sigma^x\right]\right). \quad (37)$$

In Eq. (37), $[\tilde{U}(s)]_{\mathrm{av}}$ denotes the Laplace transform of the time-development operator $U(t)$. As discussed extensively in Ref. 15, it is the physics of a given problem that decides the nature of the time-development operator. In the present context, we have adopted a system-plus-reservoir approach in order to give a proper treatment of the dissipative interaction term and systematically ''project out'' the bath degrees of freedom. This can be most conveniently achieved by writing a resolvent expansion of $[\tilde{U}(s)]_{\mathrm{av}}$ in which the interaction term H_I is treated perturbatively. Such an expansion yields the following general expression for $[\tilde{U}(s)]_{\mathrm{av}}$:[15]

$$[\tilde{U}(s)]_{\mathrm{av}}=[s-iL_s+\tilde{\Sigma}(s)]^{-1}, \quad (38)$$

where L_s is the Liouville operator associated with the spin Hamiltonian H_s, defined in Eq. (5) and $\tilde{\Sigma}(s)$ is the so-called relaxation matrix, to be specified below. While it is possible to evaluate $\tilde{\Sigma}(s)$ to arbitrary orders in perturbation theory, it suffices for the purpose of obtaining Markovian dynamics to use an expansion up to second order in H_I, which yields

$$\tilde{\Sigma}(s)=\left[L_I\frac{1}{s-iL_s-iL_B}L_I\right]_{\mathrm{av}}. \quad (39)$$

A calculation along similar lines was done by us earlier in the context of the quantum spin glass.[16] A prototypical experimental quantum spin glass is the yttrium-diluted $LiHoF_4$, viz., $LiHo_xY_{1-x}F_4$, for a concentration of $x=0.167$ (Ref. 17). Differences in the calculation arise due to an enlarged state-space in the present context, where additional degrees of freedom are present due to the inclusion of nuclear hyperfine interactions. Writing out the trace over the subsystem, we obtain using Eq. (37),

$$\tilde{C}(s)=\frac{1}{Z_s}\sum_M\sum_{\mu,\nu,\mu',\nu'}\frac{e^{\beta h(M)\mu}}{h^2(M)}\langle\mu|\tilde{H}\sigma^z-\Omega\sigma^x|\nu\rangle\times(\nu\mu|[\tilde{U}(s)]_{\mathrm{av}}|\nu'\mu')\langle\nu'|\tilde{H}\sigma^z-\Omega\sigma^x|\mu'\rangle, \quad (40)$$

where $(aM+H)$ has been denoted by $\tilde{H}$. In writing this equation, we have used the properties of the Liouville operators (refer to chapter 1 of Ref. 15) as well as the notation

$$(\mu\nu|L|\mu'\nu')=\delta_{\nu\nu'}\langle\mu|H|\mu'\rangle-\delta_{\mu\mu'}\langle\nu'|H|\nu\rangle, \quad (41)$$

where L is the Liouville operator corresponding to the Hamiltonian H. In order to make further progress we need to compute the matrix elements of $[U(s)]_{\mathrm{av}}$. The latter being a superoperator in the space of the subsystem alone, is characterized by 16 elements, because the subsystem itself is restricted to a two-dimensional Hilbert space in the present case. Using Eq. (41) the matrix elements of L_S can be written as

$$(\nu\mu|L_S|\nu'\mu')=\sum_M h(M)(\mu-\nu)\delta_{\nu\nu'}\delta_{\mu\mu'}. \quad (42)$$

Explicitly,

$$L_S=\begin{pmatrix}0&0&0&0\\0&0&0&0\\0&0&-2\sum_M h(M)&0\\0&0&0&2\sum_M h(M)\end{pmatrix}, \quad (43)$$

where the rows and columns labeled by $|\nu\mu)$ take the values $|++)$, $|--)$, $|+-)$ and $|-+)$, respectively.

The next step is the evaluation of the relaxation matrix. Treating the heat bath in the Markovian approximation, it is possible to approximate the relaxation matrix by

$$\tilde{\Sigma}(s)\approx\tilde{\Sigma}(0)=\int_0^\infty dt\,L_I(\exp[i(L_S+L_B)t])L_I. \quad (44)$$

A typical sample as evaluated from Eq. (44) is of the form

$$\begin{aligned}W_{++}&=(++|\tilde{\Sigma}(0)|++)\\&=g^2\int_{-\infty}^{+\infty}dt\left[e^{+i\sum_M h(M)t}\langle b(0)b(t)\rangle+e^{-i\sum_M h(M)t}\langle b(t)b(0)\rangle\right]\\&=g^2\Pi_M\int_{-\infty}^{+\infty}dt[e^{+ih(M)t}\langle b(0)b(t)\rangle+e^{-ih(M)t}\langle b(t)b(0)\rangle]\\&=\Pi_M W_{++}^M,\end{aligned} \quad (45)$$

where the bath correlations are defined as

$$\langle b(t)b(0)\rangle\equiv\mathrm{Tr}[\rho_B e^{iH_Bt}b(0)e^{-iH_Bt}b(0)], \quad (46)$$

ρ_B being the density operator of the heat bath. Further, the quantities W_{+-}^M and W_{-+}^M are related as

$$W_{+-}^M=e^{2\beta h(M)}W_{-+}^M. \quad (47)$$

Equation (47) expresses the detailed balance of transitions as it can be rewritten as

$$p_{-}^{\mathrm{eq}}(M)W_{+-}^{M}=p_{+}^{\mathrm{eq}}(M)W_{-+}^{M}, \tag{48}$$

where $p_{\pm}^{\mathrm{eq}}(M)$ denote the equilibrium probabilities

$$p_{\pm}^{\mathrm{eq}}(M)=\frac{e^{\pm\beta h(M)}}{e^{+\beta h(M)}+e^{-\beta h(M)}}. \tag{49}$$

Having fixed the detailed balance condition we now turn our attention to evaluating the bath correlation functions. All elements of $\tilde{\Sigma}(0)$ can be expressed in terms of certain bath correlation functions.[18] These correlations are not evaluated here explicitly but simply parametrized in terms of a phenomenological relaxation rate λ by first making use of a Kubo relation. As discussed in,[16] under the assumption that the fluctuations in the heat bath have a very short life time, λ becomes real and can be approximated by the following expression:

$$\lambda\approx\int_{-\infty}^{+\infty}dt(\langle b(t)b(0)\rangle+\langle b(0)b(t)\rangle). \tag{50}$$

Using this simplification, the matrix elements of $\tilde{\Sigma}(0)$ can be easily computed.

Coupled with Eq. (43), as worked out in detail in Ref. 16, the time development operator for the system is given by

$$[U(s)]_{\mathrm{av}}=\sum_{M}\begin{pmatrix} U_A & 0 & 0\\ & 0 & 0\\ 0 & 0 & \\ 0 & 0 & U_B\end{pmatrix}. \tag{51}$$

Here, we have substituted

$$U_A=\frac{1}{s(s+\lambda)}\begin{pmatrix} s+\lambda p_{+}^{\mathrm{eq}}(M) & \lambda p_{-}^{\mathrm{eq}}(M)\\ \lambda p_{+}^{\mathrm{eq}}(M) & s+\lambda p_{-}^{\mathrm{eq}}(M)\end{pmatrix} \tag{52}$$

and

$$U_B=\frac{1}{s(s+\lambda)+4h^2(M)}\begin{pmatrix} s+\frac{\lambda}{2}-2ih_0 & \frac{\lambda}{2}\\ \frac{\lambda}{2} & s+\frac{\lambda}{2}+2ih_0\end{pmatrix}. \tag{53}$$

We are now ready to insert Eq. (51) in Eq. (40) to get the final expression for the Laplace-transformed correlation function defined in Eq. (37)

$$\tilde{C}(s)=A\sum_{M}\left[s\frac{\tilde{H}^2}{h^2(M)}+\lambda p^2(M)\right]+\sum_{M}\frac{B\Omega^2}{h^2(M)}\left[(s+\lambda)+2ip(M)\frac{h^2(M)}{\tilde{H}}\right], \tag{54}$$

where the local polarization $p(M)$ is defined via

$$p_{+}^{\mathrm{eq}}(M)-p_{-}^{\mathrm{eq}}(M)=\frac{h(M)}{\tilde{H}}p(M)=\tanh[\beta h(M)]. \tag{55}$$

Finally, we are in a position to write an expression for the dynamic susceptibility using Eqs. (32) and (54). Comparing with Eq. (44) of Ref. 16, the dynamic susceptibility $\chi(\omega)$ for the model quantum magnet is

$$\beta^{-1}\chi(\omega)=1-\sum_{M}\frac{\left(-i\omega\frac{\tilde{H}^2}{h^2(M)}+\lambda p^2(M)\right)}{(i\omega+\lambda)}-\sum_{M}i\omega\frac{\frac{\Omega^2}{h^2(M)}\left[\lambda-i\left(\omega-2p(M)\frac{h^2(M)}{H}\right)\right]}{(\omega^2-4h^2(M))+i\omega\lambda}. \tag{56}$$

In particular, the real part of $\chi(\omega)$ is given by

$$\beta^{-1}\chi'(\omega)=1-\frac{\sum_{M}\left(\frac{\omega^2\tilde{H}^2}{h^2(M)}+\lambda^2p^2(M)\right)}{D_1}-\frac{\sum_{M}\left[\frac{\omega\Omega^2}{h^2(M)}\left(\omega-2p(M)\frac{h^2(M)}{H}(\omega^2-4h^2(M))\right)+\omega\lambda\right]}{D_2}, \tag{57}$$

while the imaginary part, related to the dissipation in the system is given by

$$\beta^{-1}\chi''(\omega)=\frac{\sum_{M}\omega\lambda\left(\frac{\tilde{H}^2}{h^2(M)}-p^2(M)\right)}{D_1}+\frac{\sum_{M}4\omega\lambda\Omega^2\left(1-\frac{\omega p(M)}{2H}\right)}{D_2}. \tag{58}$$

In Eqs. (57) and (58), $(\omega^2+\lambda^2)$ has been denoted by D_1 and $\{(\omega^2-4[h(M)]^2)+\omega^2\lambda^2\}$ by D_2, respectively. We discuss below the numerical evaluations of the real and imaginary parts of dynamical susceptibility to study the dependence on the transverse field, the temperature, and the hyperfine interactions in the forthcoming section.

VI. RESULTS AND DISCUSSION OF DYNAMICAL PROPERTIES

In Fig. 3(a), we show the numerical evaluation of the real part of the ac susceptibility χ' for temperature T of 0.2 K

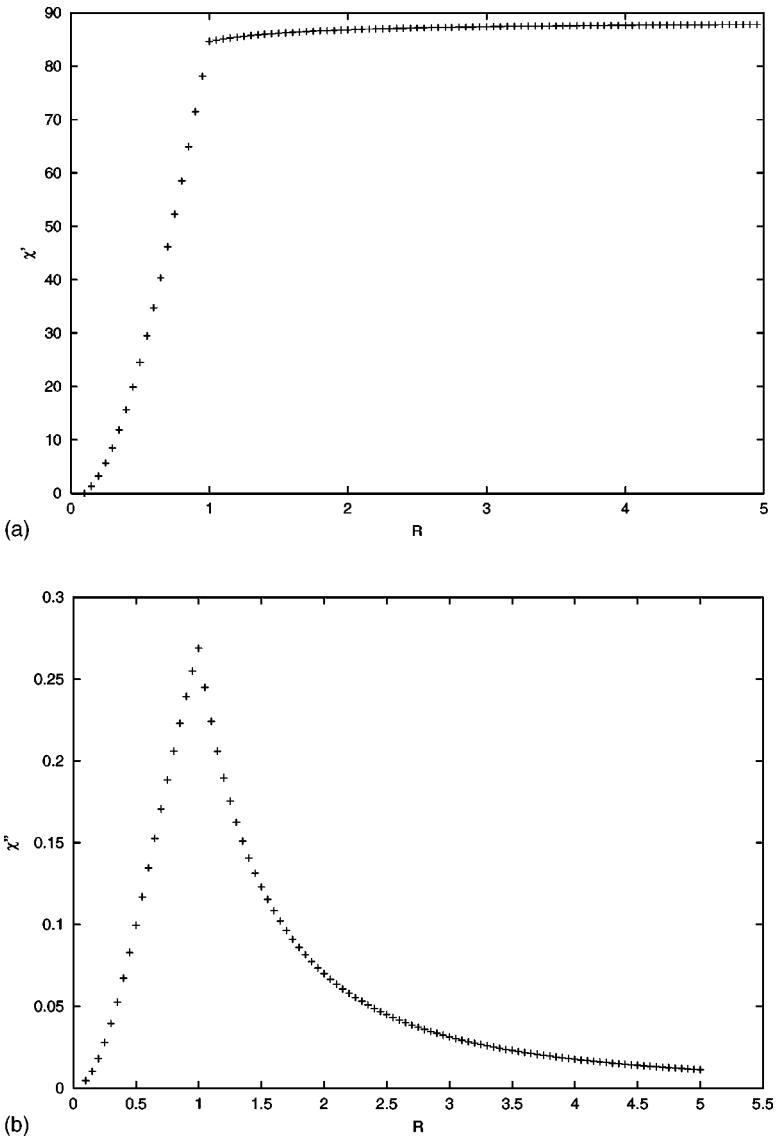

FIG. 3. (a) Numerical evaluation of the real part of the ac susceptibility, χ' for temperature T equal to 0.2 K and a frequency ω of the applied ac field equal to 0.1. R on the x axis is the ratio of $\Omega(T)/\Omega_c(T)$. (b) Imaginary part of the ac susceptibility χ'' as a function of R for the same value of T and ω as in Fig. 3(a).

and a frequency ω of the applied ac field equal to 0.1. In all numerical evaluations, we have selected the phenomenological relaxation rate λ to be 10 units. Small values of λ resulted in extremely slow relaxation as opposed to the very fast relaxation for large values of λ. However, the results presented here are fairly robust over at least a decade of λ values. The variation shown in the figure is with respect to the ratio R of the transverse field $\Omega(T)$ to the value of the critical transverse field $\Omega_c(T)$ at $T=0.2$ K. As expected, there is a sharp drop in $\chi'(R)$ at $R=1.0$. In Fig. 3(b), we plot the imaginary part of the ac susceptibility, viz., $\chi''(R)$, for the same values of T and ω as above. The sharp peak in χ'' occurs at $R=1.0$, thus coincident with the rapid drop in $\chi'(R)$, suggestive of a dynamical phase transition at $\Omega(T)=\Omega_c(T)$. We would like to comment that a similar qualitative behavior in both, $\chi'(R)$ and $\chi''(R)$ has been observed experimentally by Bitko, Rosenbaum, and Aeppli. There is, however, an important difference in that the sharp rise in χ' and the cusp in χ'' observed by them occurs at values of Ω much smaller than the corresponding values of $\Omega_c(T)$, i.e., at R values less than 1.

Figure 4 shows the variation of $\chi''(\Omega)$ for a series of temperature values ranging from $T=0.05$ K (topmost curve) where the hyperfine interaction is most effective, to 0.3 K (lower most curve) where the effect of the hyperfine interaction is small. For all values of temperature, $\chi''(\Omega)$ shows a peak at the critical field $\Omega_c(T)$, where the ferromagnetic transition occurs. We have also shown corresponding curves (dashed lines) in the absence of hyperfine interaction, for comparison. Strong differences observed for low values of temperature indicate that the presence of hyperfine interactions radically affects the response of the Ising system. As expected, the peak response shifts to higher values of the transverse field, since corresponding values of $\Omega_c(T)$ are larger in the presence of hyperfine interactions. It can also be seen that the response is quenched in the presence of hyperfine interactions. This is because the hyperfine field itself acts as a local mean field. At higher temperatures, thermal relaxational processes dominate over all other relaxational processes leading to rapid relaxation. This explains why the peak value of the response falls with increasing temperature.

Finally, in Fig. 5(a) we show the numerical evaluation of

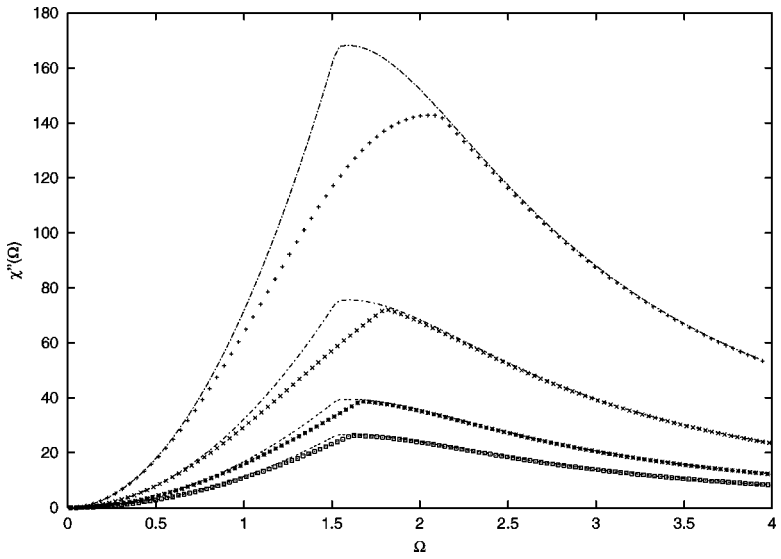

FIG. 4. Variation of $\chi''(\Omega)$ for a series of temperature values ranging from $T=0.05$ K (highest curve), where the hyperfine interaction is most effective, to 0.3 K (lowest curve) where the effect of hyperfine interaction is small. The other values of T are 0.1 and 0.2. Dashed lines are corresponding curves in the absence of hyperfine interaction.

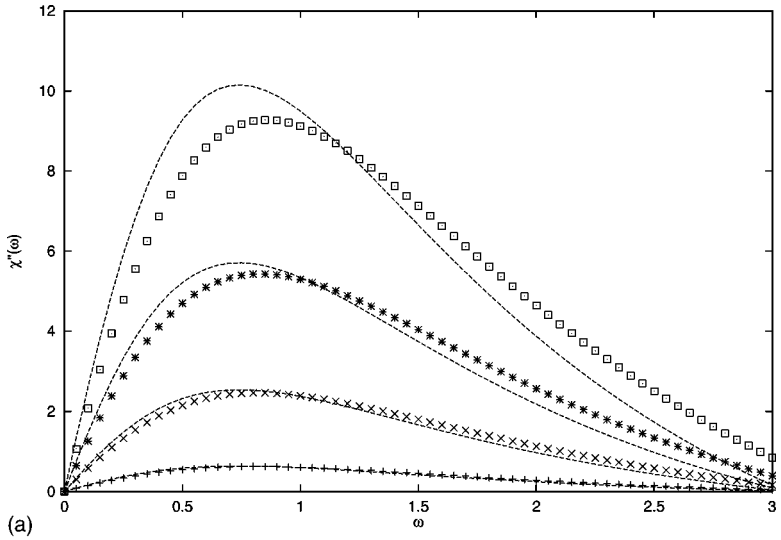

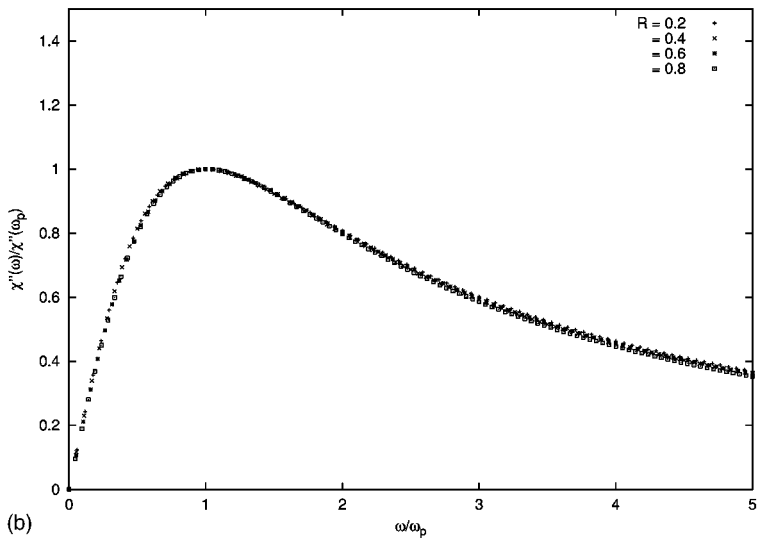

FIG. 5. (a) Evaluation of $\chi''(\omega)$ vs ω for $T=0.14$ K for values of R ranging from 0.2 (lowest curve) to 0.8 (highest curve) with an interval of $R=0.2$. Dashed lines are corresponding curves in the absence of hyperfine interactions. (b) Susceptibility curves (corresponding to presence of hyperfine interactions) of Fig. 5(a) scaled by the peak height and peak frequency i.e., $\chi''(\omega)/\chi''(\omega_p)$ vs ω/ω_p, for a set of values of R.

$\chi''(\omega)$ vs ω in the quantum limit, for a value of $T = 0.14$ K, where the hyperfine interaction term is effective. The curves correspond to different values of R ranging from 0.2 (lower most curve) to 0.8 (topmost curve). The dashed lines below each curve correspond to the evaluation of $\chi''(\omega)$ in the absence of hyperfine interactions for the same R values. There is a very important difference between the two sets of curves. We find that in the absence of hyperfine interactions, the peak value of the response occurs at the same value of frequency ($\omega = 0.09$), irrespective of the strength of the transverse field. On the other hand, on including the hyperfine interactions, we find that the peak value of the response moves to higher frequencies for higher values of the transverse field. Interestingly, such observations have been made experimentally[19,20] in the context of the yttrium diluted disordered quantum ferromagnet viz., $LiHo_{0.44}Y_{0.56}F_4$, but to the best of our knowledge, have not been reported for pure $LiHoF_4$. This signature has also been observed in $LiHo_{0.167}Y_{0.833}F_4$, which behaves as a quantum spin glass in the presence of a transverse field.[17,16] The shift in peak is purely because of the quantum mechanical nature of the system. We have checked this by evaluating $\chi''(\omega)$ vs ω for the classical ferromagnet. Thus we see that the inclusion of hyperfine interactions is crucial to mimic the relaxational behavior of a quantum magnet such as $LiHoF_4$.

We have also enquired whether the transverse field has any effect on broadening the dynamic response. In Fig. 5(b), we plot the susceptibility $\chi''(\omega)$, scaled by the peak height and peak frequency, i.e., $\chi''(\omega)/\chi''(\omega_p)$ vs ω/ω_p. There is no broadening of these curves as the transverse field is increased. Once again we point out here that such broadening effects have been seen in experiments on the disordered magnet, but have not been reported for the pure case.[20] The disordered magnet is like a quantum spin glass, in which tunneling though barriers (which are numerous) becomes a dominant mechanism of relaxation, thus resulting in broadening of $\chi''(\omega)$ with increasing transverse field.

VII. CONCLUSIONS

Techniques for studying dynamic properties of quantum systems are few and far between. Quantum Monte Carlo methods have also not been perfected for analyzing time-dependent correlation functions. In view of these difficulties, we have used a rather simple mean field approach to calculate the static phase diagram as well as the dynamic susceptibility of a model quantum magnet. We find that the transverse Ising model with hyperfine interaction term provides a valid framework for describing the physical properties of a quantum magnet such as $LiHoF_4$. The inclusion of the hyperfine interaction term in our calculations is crucial to account for experimental observations in this system. The quantum fluctuations, which speed up the relaxation processes, are manipulated in the laboratory by the application of a transverse field perpendicular to the c axis of the system. Both static as well as dynamic properties in the quantum regime show novel features explicable only by the inclusion of hyperfine interactions. We conclude that hyperfine coupling plays an important role in the low-temperature regime, which is the most interesting regime in the present context. This has motivated us to look at nuclear magnetic resonance (NMR) line shapes for quantum magnets that may shed further light on the role of hyperfine interactions. The NMR line-shape calculations are in progress and will be presented at a later date.

ACKNOWLEDGMENTS

We thank Dr. D. Bitko for sending us a copy of his Ph.D. thesis and Dr. G. Aeppli for useful discussions. V.B. is grateful to the Council of Scientific and Industrial Research of the Government of India for a research grant.

*Email address: varsha@physics.iitd.ernet.in
†Email address: sdgupta@boson.bose.res.in

[1] S. Sachdev, Phys. World **7**, 25 (1995), cond-mat/9705266; H. Reiger and A. P. Young, Lecture notes in Physics (Springer-Verlag, Heidelberg, 1996), cond-mat/9607005; R. N. Bhatt, in *Spin Glasses and Random Fields*, edited by A. P. Young (World Scientific, Singapore 1997).
[2] S. A. Carter *et al.*, Phys. Rev. Lett. **67**, 3440 (1991); Phys. Rev. B **48**, 16841 (1993).
[3] H. V. Lohneysen *et al.*, Phys. Rev. Lett. **72**, 3262 (1994); B. Bogenberger and H. V. Lohneysen, *ibid.* **74**, 1016 (1995).
[4] M. B. Maple *et al.*, J. Low Temp. Phys. **99**, 223 (1995).
[5] S. Sachdev and J. Ye, Phys. Rev. Lett. **71**, 169 (1993); A. Sokol and D. Pines, *ibid.* **71**, 2813 (1993); A. W. Sandvik and M. J. Vekic, *ibid.* **74**, 1226 (1995).
[6] D. Bitko, T. F. Rosenbaum, G. Aeppli, Phys. Rev. Lett. **77**, 940 (1996).
[7] D. D. Betts, in *Phase Transitions and Critical Phenomena*, edited by C. Domb and M. S. Green (Academic, London, 1972), Vol. 3.
[8] A. Abragam, *The Theory of Nuclear Magnetism* (Oxford University Press, London, 1961).
[9] C. P. Slichter, *Principles of Magnetic Resonance* (Harper & Row, New York, 1963).
[10] J. M. Luttinger and L. Tisza, Phys. Rev. **70**, 954 (1946).
[11] G. Mennenga, L. J. DeJongh, and W. J. Huiskamp, J. Magn. Magn. Mater. **44**, 59 (1984).
[12] K. Andres, Phys. Rev. B **7**, 4295 (1973).
[13] J. Megarino, J. Tuchendler, P. Beauvillian, and I. Laursen, Phys. Rev. B **21**, 18 (1980).
[14] K. Kawasaki, in *Phase Transitions and Critical Phenomena*, edited by C. Domb and M. S. Green (Academic, London, 1972), Vol. 2.
[15] S. Dattagupta, *Relaxation Phenomena in Condensed Matter Physics* (Academic, Orlando, 1987).
[16] V. Banerjee and S. Dattagupta, J. Phys.: Condens. Matter **10**, 8351 (1998).
[17] W. Wu, B. Ellman, T. F. Rosenbaum, G. Aeppli, and D. H. Reich, Phys. Rev. Lett. **67**, 2076 (1991); W. Wu, D. Bitko, T. F. Rosenbaum, and G. Aeppli, *ibid.* **71**, 1919 (1993).
[18] S. Dattagupta, B. Tadić, R. Pirc, and R. Blinc, Phys. Rev. B **44**, 4387 (1991); **47**, 8801 (1993).
[19] D. H. Reich *et al.*, Phys. Rev. B **42**, 4631 (1990).
[20] D. Bitko, Ph.D. thesis, University of Chicago, Illinois, 1992.